JOURNAL OF CATALYSIS 142, 226–236 (1993)

Transient Isotopic Labeling Studies under Steady-State Conditions in Partial Oxidation of Methane to Formaldehyde over MoO_3 Catalysts

M. R. SMITH[1] AND U. S. OZKAN[2]

Department of Chemical Engineering, The Ohio State University, Columbus, Ohio 43210

Received October 6, 1992; revised February 19, 1993

The oxygen insertion pathway over MoO_3 catalysts has been investigated for the partial oxidation of methane to formaldehyde using transient isotopic labeling under steady-state reaction conditions. Catalyst samples preferentially exposing basal (010) and side (100) planes have been characterized using various techniques including scanning electron microscopy with three-dimensional imaging, BET surface area, X-ray diffraction, X-ray photoelectron spectroscopy, and laser Raman spectroscopy. In addition to isotopic labeling studies, these catalysts have also been examined under steady-state reaction conditions to assess the effect of the concentration of gas-phase oxygen. Results of the characterization and reaction studies suggest that the production of HCHO proceeds via utilization of lattice oxygen through the Mo=O sites. These sites are then preferentially replenished through bulk diffusion of oxygen. The bridging Mo–O–Mo sites, on the other hand, appear to be involved in complete oxidation and are more easily regenerated by gas-phase oxygen.

INTRODUCTION

The study of the partial oxidation of methane to formaldehyde and methanol over heterogeneous catalysts has gained increasing attention in recent years as an alternative to the costly, energy-intensive steam-reforming method of production. MoO_3 is among the most widely studied systems, and has usually been studied as an SiO_2-supported catalyst, using both molecular oxygen and nitrous oxide as the oxidant (*1–6*). In studying the MoO_3/SiO_2 system using nitrous oxide, Liu *et al.* (*1*) found that the reaction is initiated by the abstraction of a H from CH_4 at O^- ions coordinated to Mo^{VI} sites. The methyl radicals formed by this abstraction rapidly react with the surface forming methoxide complexes which, in turn, decompose to HCHO or react with water to form CH_3OH. Barbaux *et al.* (*3*) have investigated the MoO_3/SiO_2 system and compared the mechanism of oxidation with both O_2 and N_2O. Using surface potential measurements, they showed that in the case of O_2 oxidant, methane is most likely attacked by adsorbed O^- species, while with N_2O oxidant, methane reacted with O^{2-} species.

Methane oxidation to formaldehyde over MoO_3/SiO_2 has also been investigated by Spencer *et al.* (*4–6*) using molecular oxygen as the oxidant. They also used HCHO and CH_3OH as feed materials over the catalyst to investigate the reaction pathway, and found that methane is directly oxidized to CO_2 and HCHO, with the further oxidation of HCHO to CO also occurring. Methanol was thought to be another possible intermediate, as traces of CH_3OH were also detected.

Several studies of the supported MoO_3 system have centered on the effect of the surface species on activity and selectivity in methane oxidation. Banares and Fierro (*7*) have used several characterization techniques to investigate the effect of MoO_3 loading and impregnation conditions on the

[1] Present address: International Paper, Mobile, Alabama 36652

[2] To whom correspondence should be addressed.

0021-9517/93 $5.00

surface species formed on the support. Smith *et al.* (*8*) have used several characterization techniques including Raman spectroscopy, X-ray photoelectron spectroscopy, and temperature-programmed reduction to investigate the surface species formed on SiO_2 at different MoO_3 weight loadings. They found that the silicomolybdic species with terminal Mo=O sites found at lower weight loadings are transformed to polymolybdate species containing Mo–O–Mo bridging sites at higher weight loadings. The loss of Mo=O sites was found to adversely affect the selectivity to HCHO.

While much work has been done on supported MoO_3 for the partial oxidation of methane, valuable information on the reaction pathway may also be gained by the study of unsupported MoO_3, as there are no catalyst/support interactions to be dealt with. Previous work by this group has shown that MoO_3 exhibits catalytic anisotropy in the partial oxidation of methane to formaldehyde (*9*). Reaction studies performed using CH_4, HCHO, CH_3OH, and CO as feed materials have shown that catalysts which exhibit a relatively larger amount of basal (010) plane are less selective to partial oxidation than those exhibiting relatively larger amounts of side (100) plane. These studies have suggested that the oxygen insertion to form HCHO took place preferentially at Mo=O sites, while CO_x formation occurred more readily at Mo–O–Mo sites. These findings also appeared to be in agreement with those conclusions drawn from the methane oxidation studies performed over silica-supported molybdenum oxide catalysts.

While previous work on MoO_3-based catalysts has provided important clues about the catalytic sites involved in partial oxidation of methane, questions still remain about the oxygen insertion pathway and the role of gas-phase vs "lattice" oxygen over these catalysts. Valuable information about the oxygen insertion pathway may be obtained by using isotopic oxygen ($^{18}O_2$) as a tracer in conjunction with a mass spectrometer for detection. Simple pulsing experiments, in which a pulse of feed mixture containing hydrocarbon and labeled oxygen is fed over a degassed catalyst can yield some information on the contribution of gas-phase and lattice oxygen (*10*). One disadvantage of this type of experiment is that it is not performed under steady-state conditions, allowing for only transient response data. An alternate isotopic labeling technique involves obtaining isotope transients under steady-state reaction conditions where the oxygen source is abruptly switched from $^{16}O_2$ to $^{18}O_2$ after steady state has been achieved (*11*). This technique has also been described in detail in application to the oxidative coupling of methane (*12–14*).

In this paper, we present the results of our investigation into the oxygen insertion pathway over MoO_3 catalysts used in the partial oxidation of methane to formaldehyde. Characterization methods included BET surface area measurement, X-ray diffraction, X-ray photoelectron spectroscopy, laser Raman spectroscopy, and scanning electron microscopy with three-dimensional imaging technique. In order to study the effect of gas-phase oxygen concentration, steady-state experiments were also performed at different oxygen concentrations over two MoO_3 catalysts with different relative basal-to-side plane areas. A set of steady-state isotopic switch experiments utilizing $^{18}O_2$ was performed over both samples to investigate the role of gas-phase vs lattice oxygen over both MoO_3 catalysts. Results from isotopic labeling studies have been combined with our previous work involving characterization and structural specificity investigations on MoO_3 catalysts to draw conclusions about the oxygen insertion scheme as well as the role of different catalytic sites.

EXPERIMENTAL METHODS

Catalyst Preparation

The MoO_3 catalysts used in these studies were prepared using temperature programmed techniques (*9*). The first sample,

denoted MoO_3-C, was prepared by calcination of MoO_3 (Aldrich) under oxygen at 675°C for 1 h. This technique produced rather thick MoO_3 crystals. The second technique used to prepare catalysts was to melt MoO_3 samples by heating them to 795°C for 12 min, then cooling rapidly to form long, thin crystallites, referred to as MoO_3-R.

Catalyst Characterization

Catalysts were characterized by several methods. The BET surface area measurements were performed using a Micromeritics Accusorb 2100E with Kr as the adsorbate. X-ray diffraction patterns were obtained using a Scintag PAD V Diffractometer and Cu K_α radiation (1.543 Å) at 45 kV and 20 mA. Raman spectra of the samples were collected using either a Spex Triplemate Raman spectrometer with CCD detector or a Spex Double Monochromator model 1403. The 514.5-nm line of a 5-W argon ion laser was used as the excitation source. X-ray photoelectron spectra were accumulated using a Physical Electronic/Perkin–Elmer model 550 ESCA/Auger spectrometer at 15 kV, 20 mA with Mg K_α radiation (1253.6 eV). Scanning electron micrographs were obtained using an Hitachi S-510 scanning electron microscope. Stereo pairs of micrographs were used in conjunction with a FORTRAN program to quantify the relative amounts of basal (010) to side (100) plane area in each sample. Details of these characterization experiments have been reported previously (9).

Reaction Studies

Steady-state reaction studies were performed using a quartz reactor consisting of a quartz tube of 5 mm i.d. at the catalyst bed portion. The bed length was held at 4.0 cm. The exit of the reactor was reduced to 2 mm i.d. to allow the gas stream to rapidly exit the heated portion of the bed. A quartz frit was used to hold the catalyst in place. The reactor temperature was maintained at 650°C by means of a stainless steel block and resistive heating cartridges. Feed streams were maintained at desired composition and flow rate by flowing methane, oxygen and nitrogen through mass flow controllers calibrated for each gas (Tylan). The total volumetric flow rate was 8.5 cm^3(STP)/min. An automated on-line gas chromatograph (HP 5890 Series II) was used in conjunction with two HP 3386A integrators for feed and product analyses. A Hayesep T column was used with both a flame ionization detector and a thermal conductivity detector for separation of CO_2, CH_3OH, HCHO, and other partial oxygenates. A molecular sieve 5A column was also used with the TCD in conjunction with a four-port valve for separation of CH_4, N_2, O_2, and CO. H_2 detection was also possible. The gas stream could also be diverted to a GC/mass spectrometer for analysis. Details of the system have been reported previously (9).

Steady-state reaction runs to assess the effect of oxygen concentration in the feed were performed at methane concentrations of 67 vol%, and the oxygen concentration was varied from 7.11 to 21.95 vol%. Nitrogen was used as an internal calibration standard for GC analysis. The reaction temperature was 650°C and pressure was 1 psig.

Transient Isotopic Labeling Experiments under Steady-State Reaction Conditions

The steady-state isotopic switching experiments were run using the reactor and feed system described above. However, a four-port valve and a second oxygen mass flow controller were included in the oxygen line. Feed composition was 67.14% CH_4, 7.11% O_2, and 25.75% He. The total feed flow rate was 8.5 cm^3 (STP)/min. After steady-state was reached, usually in 4 hours, the flow of isotopic oxygen ($^{18}O_2$, purity of 99 atom%) was started through its mass flow controller. The composition of the feed was abruptly switched from $^{16}O_2$ to $^{18}O_2$ without upsetting the steady-state by turning the four-port valve. Reactor effluent was monitored by a GC/mass spectrom-

eter (HP 5989 Mass spectrometer engine) and a Hewlett–Packard workstation. Sample was leaked to the GC/MS through a capillary column inserted in the gas stream. The experimental setup used has been previously described (*15*). The reactor effluent could also be sent to a gas chromatograph with multiple columns and flame ionization and thermal conductivity detectors for quantification of conversion and yields through the GC.

Two sets of experiments were performed over each catalyst sample, as well as over a blank reactor, all at 650°C. In the first set of experiments, no methane was present, the normal methane contribution to the feed concentration being made up by inert He. A switch from $^{16}O_2$ to $^{18}O_2$ was made, and the oxygen transients for isotopes 32, 34, and 36 were monitored. The second type of experiment was performed using the feed concentrations described above with methane present. In this case, oxygen transients, as well as transients for the products HCHO, CO_2, H_2O, and CO were monitored. Isotopic oxygen was replaced by Ar for one switching sequence over each catalyst to measure the gas-phase holdup time. Blank reactor runs were also performed to measure the relaxation time for each isotope in the absence of any catalyst.

RESULTS

Catalyst Characterization

Characterization of MoO_3-C and MoO_3-R has shown several differences in the two preparations. Three-dimensional imaging of SEM stereo pairs gave values for the basal-to-side-plane area ratio of 3.5 and 6.5 for MoO_3-C and MoO_3-R, respectively. The BET surface area of MoO_3-C was 0.32 m^2/g, while that of MoO_3-R was 0.12 m^2/g.

X-ray diffraction patterns of the two samples provided additional evidence of the preferred exposure of different crystal planes through significant differences in the relative intensities of the diffraction bands resulting from (0*k*0) and (*h*00) planes. The unit cell dimensions for the orthorhombic system are chosen as a = 3.9639, b = 13.856, c = 3.6996 Å. The details of these results have been presented earlier (*9*).

Raman spectra have also reflected the differences in the MoO_3 samples, the most noticeable being in the relative intensity of the bands associated with Mo=O and Mo–O–Mo stretching vibrations (818 and 995 cm^{-1}, respectively). The bands associated with Mo–O–Mo sites were seen to be considerably more intense relative to bands which are due to terminal oxygen sites in samples which had a larger percentage of the (010) plane area. Similar trends were observed at low-wavenumber bands which are assigned to deformation of bridging and terminal oxygen bonds (*9*).

Reaction Studies

Results of steady-state reaction experiments to assess the effect of gas-phase concentration of oxygen in the feed stream are shown in Fig. 1. From the figure, it is seen that over both catalysts, the selectivity to HCHO decreases while the CO_2 selectivity

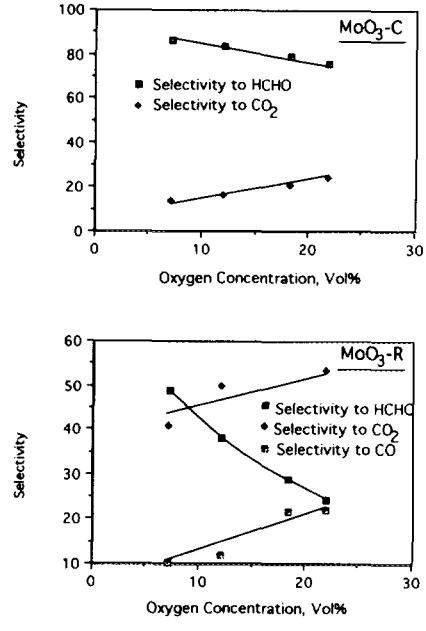

FIG. 1. Effect of oxygen concentration on product selectivities.

increases with increasing O_2 concentration. However, this trend was more pronounced over MoO_3-R than over MoO_3-C. Also, formaldehyde was the major reaction product over MoO_3-C at every oxygen concentration level, while, over MoO_3-R, CO_2 selectivity is higher than HCHO selectivity with the exception of the lowest O_2 level, where the selectivity to HCHO is slightly higher than the selectivity to CO_2. Finally, it is noted that over MoO_3-R, the change in HCHO selectivity was strongly dependent on oxygen concentration, while the changes in selectivity for CO_2 and CO were more gradual.

Transient Isotopic Labeling Experiments under Steady-State Reaction Conditions

The oxygen isotope transients obtained by switching from $^{16}O_2$ to $^{18}O_2$ in the gas phase without any methane present are shown in Fig. 2 for MoO_3-C and MoO_3-R. The transients are presented for the first 5 min, although data were collected for a total of 16 min. The isotope signals have been normalized so that the sum of the signals from isotopes 32 ($^{16}O^{16}O$), 34 ($^{16}O^{18}O$), and 36 ($^{18}O^{18}O$) is unity. An interesting feature of the transient data is that the signals for $^{16}O^{16}O$ and $^{16}O^{18}O$ do not relax all the way to zero, but continue at a nonzero level representing a "pseudo-steady-state" involvement of the lattice oxygen. When the $^{16}O^{16}O$ transients are compared for the two catalysts, it is seen that the pseudo-steady-state value over MoO_3-R is greater than that over MoO_3-C. The pseudo-steady-state signal for $^{16}O^{18}O$, although relatively small, is larger over MoO_3-R than over MoO_3-C. When similar oxygen switching experiments were performed with a blank reactor, the relaxation of $^{16}O_2$ transient was almost instantaneous, following that of the inert very closely. These experiments showed that the interaction of oxygen with the reactor surfaces was not a factor in isotopic transients. These experiments also showed that the nonzero signals for $^{16}O_2$ and $^{16}O^{18}O$ that continued for several minutes after the switch were not due to the presence of ^{16}O as an impurity in the $^{18}O_2$ stream. The transient relaxation time for an inert of the same concentration as the oxygen was also determined in a separate switch from Ar to $^{16}O_2$. This represents the gas-phase holdup over the catalyst bed (Fig. 3).

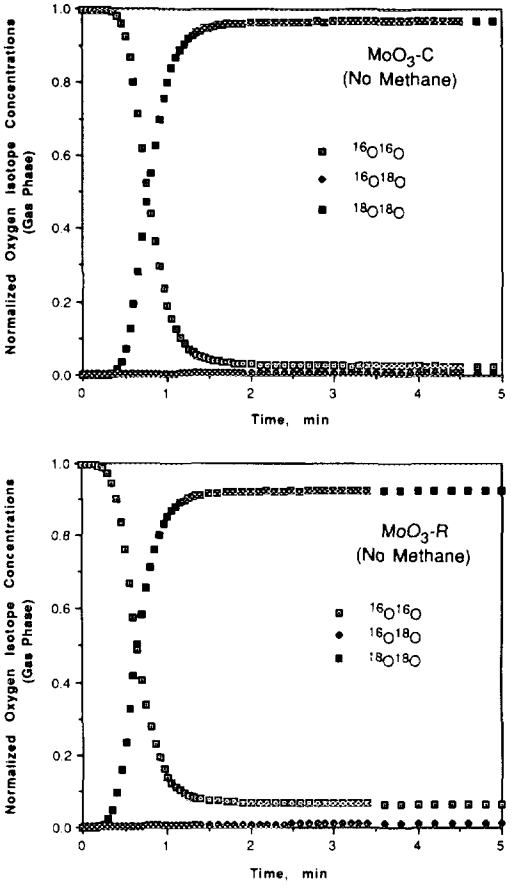

FIG. 2. Normalized isotope concentrations for oxygen without methane.

The total flux of ^{16}O into the gas phase (μmol/m^2-min) is plotted by combining the ^{16}O contribution of the signals from $^{16}O^{16}O$ and $^{16}O^{18}O$ and using the oxygen flow rate (Fig. 4). One major difference between the total ^{16}O transients for the two catalysts is in the "pseudo-steady-state" value at times greater than 1.5 min. At this point in time, all of $^{16}O_2$ originally present in the gas stream has already exited the reactor, so

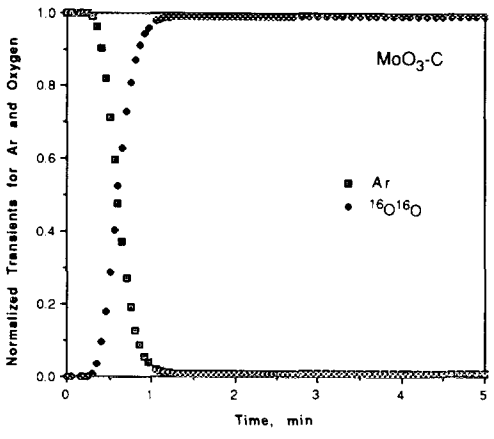

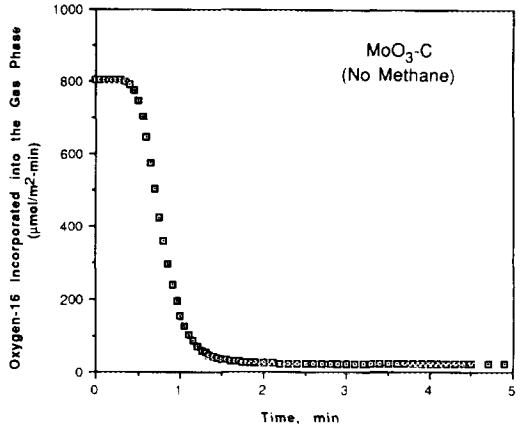

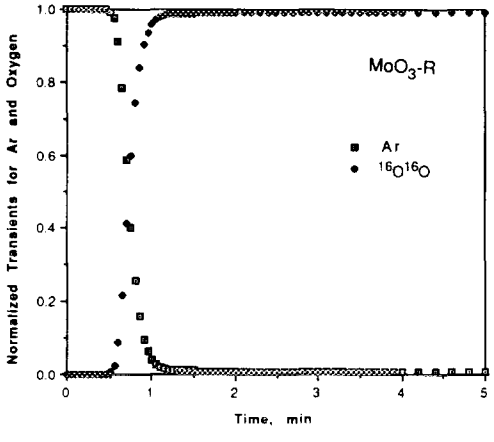

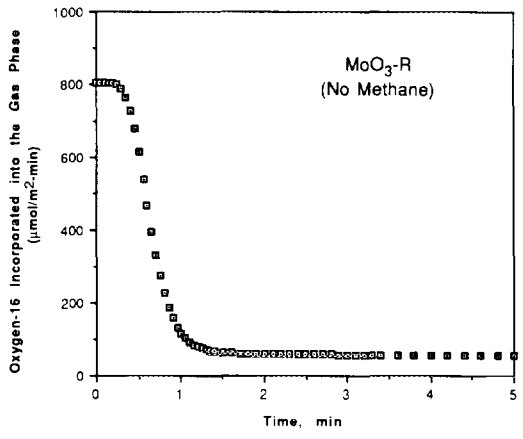

FIG. 3. Gas-phase holdup measurements through inert relaxation.

FIG. 4. Total flux of ^{16}O into the gas phase without methane.

the only continuing source for ^{16}O contribution is desorption/exchange from the catalyst surface. The total amount of ^{16}O that was incorporated into the gas phase over 16 min, through either desorption of surface oxygen, or through oxygen exchange, was calculated by integrating the area under the curve and correcting for the gas-phase holdup (Table 1). The amount of readily available surface/subsurface oxygen atoms was also calculated by correcting this value for the pseudo-steady-state contribution

TABLE 1

Comparison of ^{16}O Incorporation into the Gas Phase with No Methane Present

Catalyst	Total ^{16}O incorporated into the gas phase (over 16 min)	Total ^{16}O incorporated into the gas phase[a] (over 16 min)	Pseudo-steady-state ^{16}O incorporation rate at the 16th min
MoO_3-C	2.88×10^{20} atoms/m^2	1.02×10^{20} atoms/m^2	1.25×10^{19} atoms/m^2-min
MoO_3-R	5.88×10^{20}	1.73×10^{20}	2.85×10^{19}

[a] Corrected for pseudo-steady-state contribution.

from the bulk of the catalyst. These values are shown in Table 1 along with the pseudo-steady-state ^{16}O incorporation rate. Comparison between the catalysts shows that MoO_3-R is desorbing/exchanging more oxygen atoms than is MoO_3-C.

Similar isotope switching experiments were performed under steady-state reaction conditions. The methane conversion levels were 1.3 and 1.6% for MoO_3-C and MoO_3-R, respectively. Normalized oxygen transients obtained during steady-state methane oxidation experiments did not show major differences between the two catalysts. One other interesting point about these experiments was that the total contribution from ^{16}O declined much more rapidly and the "pseudo-steady-state" concentration of ^{16}O in the gas phase was much smaller compared to the case where there was no methane present in the reactor.

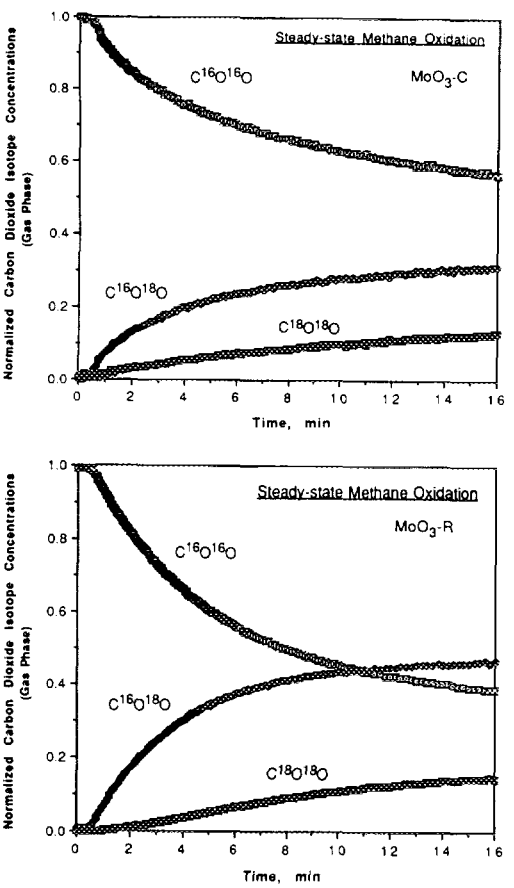

FIG. 5. Normalized isotope concentrations for carbon dioxide during steady-state methane oxidation.

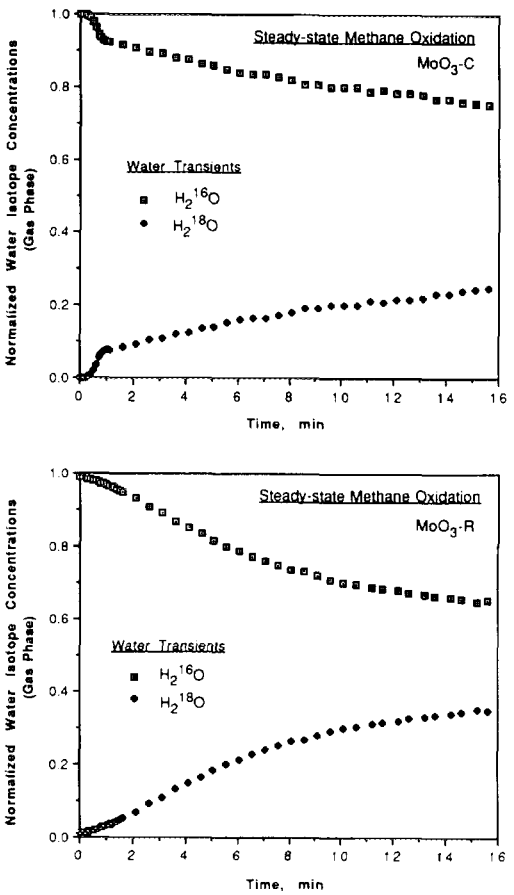

FIG. 6. Normalized isotope concentrations for water during steady-state methane oxidation.

The normalized product transients were also obtained for steady-state methane oxidation runs. The CO_2 transients are shown in Fig. 5 for MoO_3-C and MoO_3-R. Over both catalysts, the signal for the mixed isotope, $C^{16}O^{18}O$, was greater than that for the $C^{18}O^{18}O$ throughout the duration of the transient experiment. The normalized transients for water isotopes over MoO_3-C and MoO_3-R are shown in Fig. 6. While the transients show that ^{18}O was being incorporated into water, the decay of the $H_2{}^{16}O$ signal and the rise in the $H_2{}^{18}O$ signal were gradual.

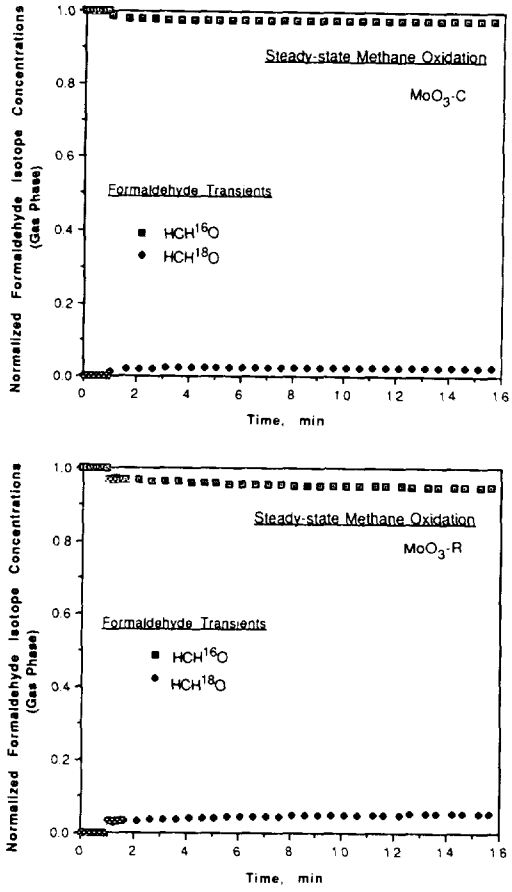

FIG. 7. Normalized isotope concentrations for formaldehyde during steady-state methane oxidation.

Transients were also plotted for formaldehyde and CO, and are shown in Figs. 7 and 8. The MoO_3-C catalyst did not show any quantifiable CO production. The most striking observation about the HCHO transients is that they did not show much ^{18}O incorporation for HCHO over the duration of the transient experiment, even though HCHO was the major product over MoO_3-C. The CO transients show that there was some incorporation of ^{18}O into CO, however, the decay rate for $C^{16}O$ was much slower than that for $C^{16}O^{16}O$.

By combining the rate of formation of each product with normalized transient isotope signals, it was possible to quantify the amount of ^{16}O incorporated into each product. Percentages of ^{16}O incorporated into each product at the 16th minute are shown in Table 2. This table shows oxygen incorporated into HCHO to consist almost exclusively of ^{16}O, while the percentages for CO_2 and H_2O are substantially lower. Under reaction conditions, when methane is present, the total ^{16}O incorporation into the gas phase over MoO_3-R is still higher than that over MoO_3-C. This is shown in Table 3, where the total amount of ^{16}O incorporated into the gas phase, in the form of products or molecular oxygen, over 16 min is presented after correction for gas-phase holdup. Values corrected for pseudo-steady-state contribution as well as the pseudo-steady-state ^{16}O incorporation rate are also shown. It is interesting to note the pseudo-steady-state value for the ^{16}O incorporation rate is still higher over MoO_3-R than over MoO_3-C, although over MoO_3-C the rate has increased from the rate with no

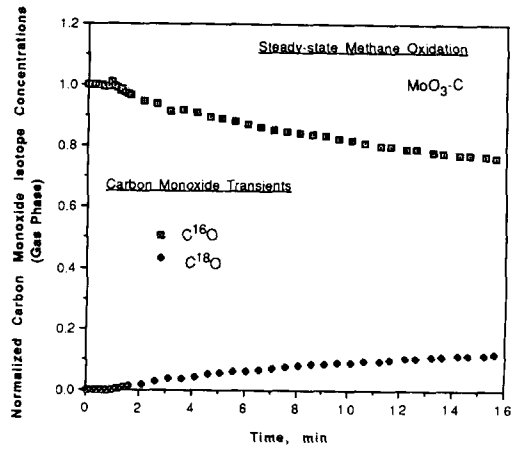

FIG. 8. Normalized isotope concentrations for carbon monoxide during steady-state methane oxidation.

TABLE 2

Percentage of ^{16}O Incorporated into Products at the 16th Min

Catalyst	CO_2	H_2O	HCHO	CO
MoO_3-C	71.5	73.8	97.5	
MoO_3-R	61.6	65.3	94.8	86.2

TABLE 3

Comparison of ^{16}O Incorporation into the Gas Phase under Steady-State Methane Oxidation Conditions

Catalyst	Total ^{16}O incorporated into the gas phase (over 16 min)	Total ^{16}O incorporated into the gas phase[a] (over 16 min)	Pseudo-steady-state ^{16}O incorporation rate at the 16th min
MoO_3-C	3.02×10^{20} atoms/m^2	3.58×10^{19} atoms/m^2	1.81×10^{19} atoms/m^2-min
MoO_3-R	4.88×10^{20}	1.25×10^{20}	2.40×10^{19}

[a] Corrected for pseudo steady-state contribution.

methane present, while over MoO_3-R, the rate has decreased slightly from the rate with no methane present.

DISCUSSION

When the results from our previous characterization and catalytic anisotropy investigations on MoO_3 crystals are considered in conjunction with the transient isotopic labeling studies under reaction conditions, important clues are obtained about the catalytic role of different oxygen sites and the oxygen insertion scheme in partial vs complete oxidation of methane.

Different thermal treatment techniques led to the growth of MoO_3 crystals which preferentially exposed (010) or (100) planes. While scanning electron microscopy images provided the visual evidence for varying crystal size and dimensions, three-dimensional imaging technique allowed for accurate quantification of these crystal planes. The differences in crystal dimensions were also verified by X-ray diffraction technique.

Another important feature observed in the characterization of these catalysts was the change in the relative intensity of the Raman bands associated with stretching and deformation vibrations of Mo=O and Mo–O–Mo sites. The samples with a larger percentage of the (010) planes gave higher relative intensities for vibrations associated with bridging oxygen sites. When the crystal structure of MoO_3 is considered, the (010) plane is seen to contain three different oxygen sites, one being a terminal oxygen site, and the other two being "double-bridging" and "triple-bridging" oxygen sites (*16*, *17*). On the (100) face, on the other hand, the Mo=O site density is much higher than it is on the basal plane. There are no Mo–O–Mo sites present on this plane, the only bridging oxygen sites being shared by three molybdenum octahedral centers. Another point that should be noted is that the terminal oxygen sites present on (010) and (100) planes are not only different from one another in site density, but also in bond length and the angle they make with the crystal plane in question due to the distorted nature of MoO_3 octahedra. These considerations lead us to suggest that the catalytic performance differences observed over these MoO_3 crystals, which preferentially expose different crystal planes, are due to the relative abundance of the Mo=O and Mo–O–Mo sites exposed on these samples.

While TPR experiments showed the sites on (010) planes to reduce more readily, the steady-state-reaction conditions showed a strong dependence of HCHO selectivity on the relative abundance of (100) planes (*9*). These observations, when combined with the results from previous studies on SiO_2-supported molybdena catalysts (*8*) seem to suggest that HCHO formation takes place on the Mo=O sites, whereas Mo–O–Mo sites promote complete oxidation more readily. Our previous results (*9*), which showed that HCHO formation rates normalized with respect to the surface area of the (100) planes were equal for the two cat-

alysts, reinforce this hypothesis. If this argument is extended to the silica-supported catalysts, it can be said that the major role of the silica support is to help the formation of silica molybdic species exposing Mo=O sites at low loading levels.

The transient isotopic labeling studies performed under steady-state reaction conditions provided some very important clues about the way oxygen is incorporated in the formation of formaldehyde. As mentioned before, this technique is a powerful tool in following isotopic tracers without disturbing the steady state once it is established. The most noteworthy feature of these results is the rate of ^{16}O incorporation into the HCHO molecule well after the $^{16}O_2$ present in the gas phase has exited the reactor. As shown in Table 2, even after 16 min following the switch of gas phase oxygen source from $^{16}O_2$ to $^{18}O_2$, the oxygen used in the formation of HCHO is almost exclusively ^{16}O (~98%). At this point in time the only continuing source of ^{16}O in the reactor is the catalyst lattice. This clearly indicates that oxygen incorporation into HCHO takes place on the catalyst surface using lattice oxygen. Another important point that should be noted is that at 16 min, the total ^{16}O incorporated into products is equivalent to using between 13–30 layers of "surface/subsurface" oxygen. Hence, this high percentage of ^{16}O incorporation cannot be explained by O atoms which may have been chemisorbed to the surface. This evidence suggests not only that oxygen incorporation into HCHO takes place on the catalyst surface, but also that the replenishment of the reduced oxygen sites used in HCHO formation is achieved primarily by diffusion of bulk oxygen to the surface from the catalyst lattice. If the assumption that HCHO formation takes place on the Mo=O sites located on (100) planes is true, this would also mean a rapid reoxidation of these sites by bulk diffusion from the lattice.

Our previous *in situ* laser Raman spectroscopy studies combined with isotopic labeling technique provide evidence which support this possibility (9). When an MoO_3 sample was reduced by limiting the reduction as close to the surface as possible, both the 818- and 995-cm^{-1} bands were substantially reduced in intensity. After the sample was brought into contact with $^{18}O_2$ in the gas phase for a short period of time, the band associated with Mo=O sites was seen to gain its original intensity without showing any shift or band broadening, whereas the band due to Mo–O–Mo sites was seen to gain only part of its prereduction intensity while showing a small shift in the position and, more importantly, showing close to 33% increase in full band width at half height. This evidence seems to suggest that Mo–O–Mo site are more easily replenished with gas-phase oxygen than Mo=O sites. On the other hand, reduced Mo=O sites seem to be reoxidized by diffusion from the catalyst lattice. Similar conclusions were drawn when the catalysts were reduced *in situ* and allowed to sit in an inert atmosphere without being exposed to any gas-phase oxygen. This experiment also showed that oxygen diffusing from the bulk was an important factor in replenishment of certain sites in MoO_3.

The steady-state reaction studies, where the effect of gas-phase oxygen was investigated, have indicated that MoO_3-R is much more sensitive to the gas-phase oxygen concentration than is MoO_3-C, although increased oxygen concentration adversely affects the HCHO selectivity over both catalysts. As CO_2 is the major product over MoO_3-R, this suggests a stronger involvement of gas-phase oxygen in formation of CO_2 although it is very likely that CO_2 formation takes place through a network of multiple reactions. CH_4 could be directly oxidized to CO_2, although the number of oxygen insertion steps would make this direct pathway unlikely. HCHO and CO may also further oxidize to form CO_2. The formation of CO_2 may involve either lattice or gas-phase oxygen. The steady-state isotopic switch experiments have shown that the ^{18}O incorporation to CO_2 is larger than

in any other product although ^{16}O incorporation was still significant (Table 2). Although this evidence would not completely rule out the presence of an Eley–Rideal type mechanism where, for example, HCHO on the surface is oxidized by gas-phase oxygen, it is more likely that the predominant step for CO_2 formation involves a surface oxygen site, possibly the Mo–O–Mo site on the (010) plane, which appears to be replenished preferentially by gas-phase oxygen. It should be noted that there is evidence of partial reoxidation of Mo–O–Mo sites by bulk diffusion of oxygen as well. However, it appears that Mo=O sites are reoxidized more easily with lattice oxygen diffusion than bridging oxygen sites. This could be due to a faster oxygen diffusion rate along the c-axis of the catalyst lattice, possibly because of the chain forming structure of MoO_3 along this axis. It should also be noted that further study is needed on the secondary oxygen exchange of carbon dioxide, since this phenomenon could also be affecting the relative distribution of labeled and unlabeled oxygen in CO_2, as reported in the literature (*18*, *19*), and studies are currently underway to examine this interaction.

ACKNOWLEDGMENTS

The financial support from National Science Foundation through Grant CTS-8912247 is gratefully acknowledged. The authors also acknowledge Ms. Sharon A. Driscoll for her technical assistance in the isotopic labeling experiments.

REFERENCES

1. Liu, H.-F., Liu, R.-S., Liew, K. Y., Johnson, R. E., and Lunsford, J. H., *J. Am. Chem. Soc.* **106,** 4117 (1984).
2. Khan, M. M., and Somorjai, G. A., *J. Catal.* **91,** 263 (1985).
3. Barbaux, Y., Elamrani, A., and Bonnelle, J. P., *Catal. Today* **1,** 147 (1987).
4. Spencer, N. D., and Pereira, C. J., *AIChE J.* **33,** 1808 (1987).
5. Spencer, N. D., *J. Catal.* **109,** 187 (1988).
6. Spencer, N. D., Pereira, C. J., and Grasselli, R. K., *J. Catal.* **126,** 546 (1990).
7. Banares, M. A., and Fierro, J. L. G., *in* "Preprints, ACS Catalytic Selective Oxidation Symposium," Vol. **37,** No. 4, p. 1171. Am. Chem. Soc., Washington, DC, 1992.
8. Smith, M. R., Zhang, L., Driscoll, S. A., and Ozkan, U. S., *Catalysis Letters*, in press.
9. Smith, M. R., and Ozkan, U. S., *J. Catal.*, **141,** 124 (1993).
10. Ozkan, U. S., Driscoll, S. A., Zhang, L., and Ault, K. L., *J. Catal.* **124,** 183 (1990).
11. Biloen, P., Helle, J. N., van den Berg, F. G. A., and Sachtler, W. M. H., *J. Catal* **81,** 450 (1983).
12. Peil, K. P., Goodwin, J. G., Jr., and Marcelin, G., *J. Phys. Chem.* **93,** 5977 (1989).
13. Peil, K. P., Goodwin, J. G., Jr., and Marcelin, G., *J. Catal.* **131,** 143 (1991).
14. Peil, K. P., Goodwin, J. G., Jr., and Marcelin, G., *J. Catal.* **132,** 556 (1991).
15. Driscoll, S. A., Zhang, L., and Ozkan, U. S., *in* "Catalytic Selective Oxidation" (S. T. Oyama, J. W. Hightower, Eds.), p. 340. Am. Chem. Soc., Washington, DC, 1993.
16. Kihlborg, L., *Ark. Kemi* **21**(34), 357 (1963).
17. Haber, J., and Serwicka, E. M., *React. Kinet. Catal. Lett.* **35**(1), 369 (1987).
18. Matsuura, I., and Kirishiki, M., *Chem. Lett.*, 1441 (1986).
19. Koranne, M. M., Goodwin, G. J., and Marcelin, G. *in* "Preprints of the 10th International Congress on Catalysis," p. 14, Institute of Isotopes of the Hungarian Academy of Sciences, Budapest, 1992.